Acta Scientiarum
http://periodicos.uem.br/ojs
ISSN on-line: 1807-8664
Doi: 10.4025/actascitechnol.v44i1.56069

Kinematic model of bar mechanism for ectrodactyly applications

Jesse Alexander Caicedo[1], Angie Julieth Valencia[2], Oscar Fernando Avilés Sanchez[1*], Mauricio Felipe Mauledoux[1] and Max Suell Dutra[2]

[1]Davinci Research Group, Mechatronics Engineering Department, Militar Nueva Granada University, Carrera 11, Nº 101-80, Bogotá, Colombia. [2]Laboratório de Robótica, Departamento de EngenhariaMecânica, Universidade Federal do Rio de Janeiro, Rio de Janeiro, Rio de Janeiro, Brasil. *Author for correspondence. E-mail: oscar.aviles@unimilitar.edu.co

ABSTRACT. This document describes the design and construction of a mechanical device that allows a subject with ectrodactyly to perform a power grip. For this purpose, the coupled bar mechanism for the emulation of a finger is presented, and a system that allows, from a single movement, to perform a large diameter grip, considering design variables obtained from anthropometric and goniometric measurement techniques. This is complemented by kinematic and static analysis, in which the position and force behaviours required in the design are verified. Then, the final construction scheme is carried out by means of computer-assisted design (CAD) software, in which the position behaviour of the distal phalanx end is obtained and compared with the models obtained in Linkage and Matlab. Finally, the work conclusions are presented.

Keywords: Bar mechanisms; taxonomy; ectrodactyly; mechatronic device; prosthesis.

Received on October 2, 2020.
Accepted on March 26, 2021.

Introduction

The term ectrodactyly (lack of fingers) derived from the Greek ektroma (abortion) and daktylos (finger), is manifested as an autosomal dominant hereditary disorder with incomplete penetrance and variable expressivity, which modifies the gen TP63 and the chromosomes 2, 7, 10, or X (Jindal, Parmar, & Gupta, 2009), (Sutton, & Van Bokhoven, 1993), (Kalathia, Seta, & Parmar, 2013). Ectrodactyly affects approximately 1 in 90,000 to 150,000 live births with prenatal diagnosis established by obstetric ultrasound in the second trimester of pregnancy (Gane & Natarajan, 2016).

This disorder causes anomalies in the human limbs involving the central rays of the autopod and it is observed as: partial or total absence of the fingers, syndactyly, or finger or toe fusing; often described as "claw-like or lobster claw hand", with greater incidence in the upper limbs compared to the lower ones (Nunes, Jadan, & Bello, 2014), (Jindal et al., 2009). The hand malformation is classified in two basic subtypes: typical form (1 in 90,000) in which the metacarpal bones and phalanges are absent, dividing the hand into ulnar and radial portion (V-shaped defect); and atypical (1 in 150,000) where the metacarpal bones generate a wide fissure (U-shaped defect) (Nirmala, Sandeep, Chaitanya, Nuvvula, & Veluru, 2015), (Bharati et al., 2020).

In Colombia, congenital anomalies generate more than 30% of the disability in the general population, which includes congenital cardiopathies (15.73 in 10,000 live births), Down's syndrome (17.82 in 10,000 live births), cleft lip and palate, and neural tube closure defects. For their follow-up, the national public health surveillance system and the SIVIGILA information subsystem created a congenital defect notification in which the pathologies presented by newly born in the city of Bogotá are recorded. From this information, it is observed that in 2012, 2 cases of ectrodactyly were reported, in 2013 there were 3 cases, and for 2014 and 2018 there was 1 case (Avila, 2018; França Bisneto, 2012).

From a biomechanical point of view, patients with ectrodactyly are very affected since they have at least one or two fingers that supply basic gripping functions. This accompanied by orthopedics, which offers orthotics to improve interaction with the environment, as well as to prevent deformations and make physical corrections; or rehabilitation that helps improve the maneuverability of the hand with existing fingers. It should be noted that the method of rehabilitation or orthotics varies from individual to individual since the malformations differ in size, shape, number of fingers, among others (Valderrama-Zaldivar, 2013).

In terms of mechanical solutions, there is a series of systems to improve the ranges of movement in the hands of people with ectrodactyly. Then, full hand prosthetic mechanism is made, which eliminates movement in the existing fingers, controlled by physiological signals or movements in different parts of the upper limb such as the wrist and/or forearms. Some of these systems are based on pulley or gears mechanisms, such as the Vincent evolution 2 and the system created by the company I-limb or linkage systems such as those presented by Bebionic and Vincent that show four ways of moving a finger from different bar configurations (Belter, Segil, Dollar, & Weir, 2013), (Van Der Niet, Bongers, & Van Der Sluis, 2013), (Belter et al., 2013), or others such as the one presented by P&G MG LATAM in (P&O MG LATAM, 2020), which reports the treatment of ectrodactyly from silicone prostheses. Finally, (Jabin, Adnan, Mahmud, Chowdhury, & Islam, 2019) show a cost-effective prosthesis for an upper limb congenital amputee patient using 3D printing technology.

As seen above, the current systems eliminate the functionality of the existing fingers in people with ectrodactyly and create mechanisms whose operation is based on other types of control signals, leading to possible muscle atrophy or increased malformation.

Therefore, the main contribution of this work is the development of a prosthesis for a person with ectrodactyly that requires power gripping using the existing fingers on the right hand since currently there are no devices on the market that can be coupled for this type of pathology. Furthermore, since this malformation is rare, the designs must be customized considering the type of defect (U or V), the fingers that are missing, and the hand size.

Material and methods

For the development of the present work, a crossbar mechanism is proposed in Figure 1, which allows obtaining behaviors of force and position necessary to supply power grips, involving a maximum of one actuator per finger. Furthermore, its functionality and aesthetics emulate the natural finger movement in a similar way. From here, the finger can be observed in extension, flexion, and intermediate positions, as well as the trajectory of the distal phalanx end.

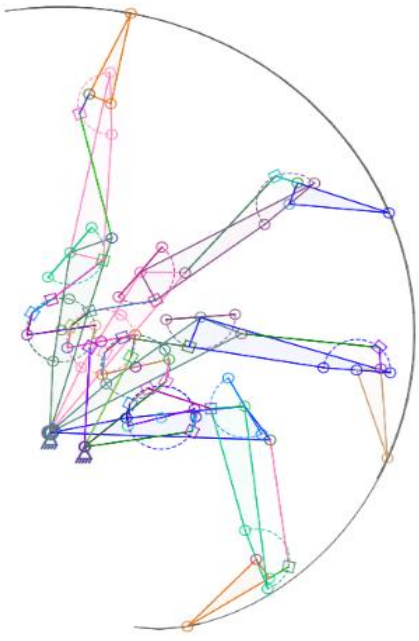

Figure 1. Bar mechanism for finger emulation.

Taxonomy of Grasp

Determining the anatomical behavior of the hand makes it possible to establish variables of force and angles of movement, which are the basis for structures that enable behaviors like those of the human hand. For this reason, the design begins by proposing the form of the power grip to be worked on based on the Cutkosky taxonomy in Figure 2 (Cutkosky, 1989). From there, the grips that a person with ectrodactyly can make are highlighted in red, and the power grip that the mechanism must make is highlighted in green.

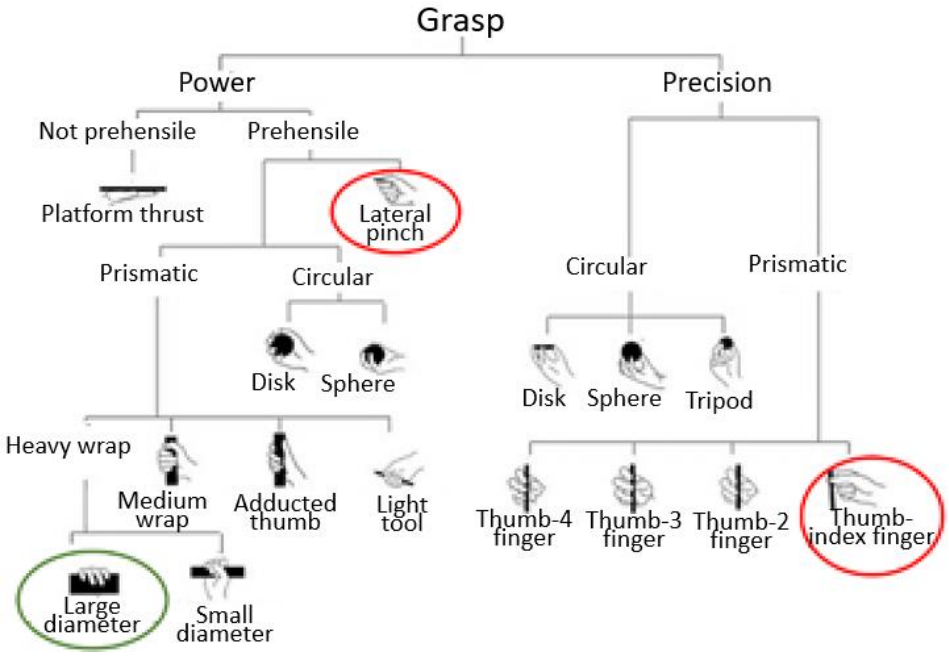

Figure 2. Cutkosky's taxonomy.

Anthropometric considerations for subjects with ectrodactyly

For the development of the prosthesis, the anthropometric measurements of the healthy hand of a test subject are considered; this, to handle a dimensional relationship between the healthy hand and the designed hand. based on this, the following design variables are considered.

Healthy hand dimensions

As main dimensions we take the measurements of the proximal and distal phalanx of the little finger and index finger, as shown in Figure 3. From this we get that the thickness of the proximal and distal phalanx of the little finger is 35.2 and 24 mm, respectively; while, for the proximal and distal phalanx of the index finger we have dimensions of 44 and 30 mm, respectively.

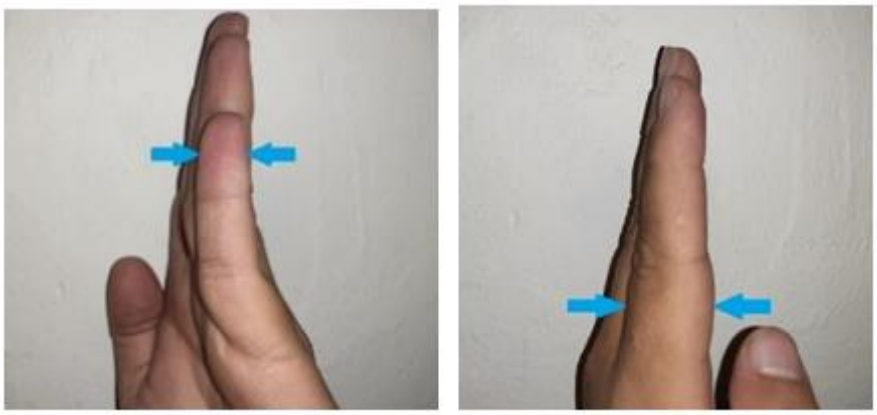

Figure 3. Side view of the fingers, hand without pathology.

Hand dimensions with ectrodactyly

The purpose of taking anthropometric measurements of the hand of the subject with ectrodactyly is to define the working space for the prosthesis drive system. Therefore, in Figure 4, the affected hand is shown, as well as the schematic dimension of the general dimensions (height and width) of the hand.

Design of the bar mechanism

With the data obtained, both from the hand anatomy and the anthropometric dimensions, the design of the bar mechanism is approximated by means of the graphic method in the Linkage software, shown in Figure 5.

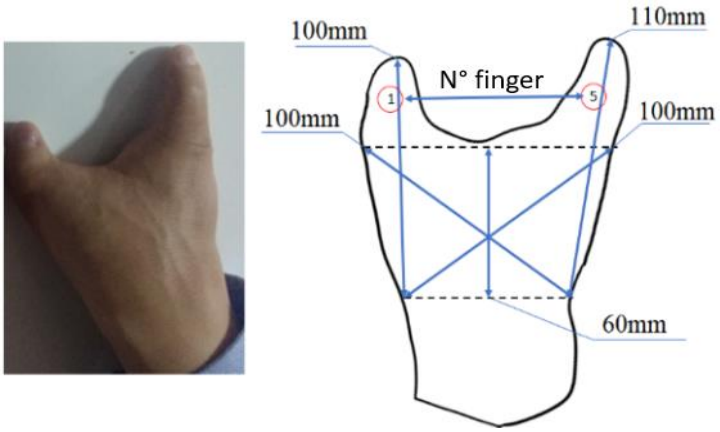

Figure 4. Hand with ectrodactyly.

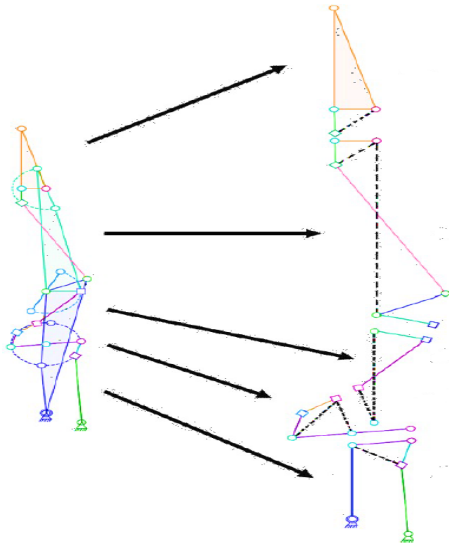

Figure 5. Graphic method by Linkage software.

With the established design, the kinematic calculation is carried out to obtain the angular variables involved in the movement of the mechanism. For this purpose, it was subdivided into simplified configurations of four and three bars. It must be considered that the selection of the independent sets depends on the phalanx to be emulated, as well as on the dimensions of each one. For the proximal phalanx, the measures are 28.3 mm, for the middle phalanx of 24 mm, and for the distal phalanx of 20 mm, the above having as reference the index finger, for the other fingers the dimensions are scaled.

The first configuration is shown in Figure 6, which is defined as an articulated quadrilateral type of mechanism. It should be taken into account that the mechanism built does not have the dotted line but the BH and HF bars do not modify the angle between them, so a scalene triangle can be formed to simplify the calculations.

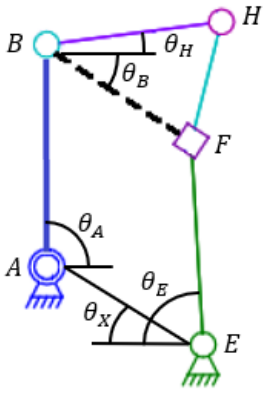

Figure 6. Initial bar configuration, input by the AB link.

The system of Figure 7 is worked in vector form, so the loop closing equation is presented in Equation (1) and (2). Then, in Equations (3) and (4) the Freudenstein equations described for the solution of four-bar mechanisms are implemented, from which the value of θ_B is obtained, knowing θ_A as the angle of entry and θ_X ,which is known from the geometry of the finger and whose value is 23.8°.

$$AB\cos\theta_A + BF\cos\theta_B + FE\cos\theta_E - EA\cos\theta_X = 0 \quad (1)$$

$$AB\sin\theta_A - BF\sin\theta_B - FE\sin\theta_E + EA\sin\theta_X = 0 \quad (2)$$

$$FE^2\cos^2\theta_E = (EA\cos\theta_X - AB\cos\theta_A - BF\cos\theta_A)^2 \quad (3)$$

$$FE^2\sin^2\theta_E = (EA\sin\theta_X + AB\sin\theta_A - BF\sin\theta_B)^2 \quad (4)$$

Where AB equals 16 mm, FE = 15.5 mm, BF = 5 mm, AE = 5.5 mm. Equalizing Equations (3) and (4), Equation (5) is obtained, which finally allows us to obtain the value θ_B, which will be the starting pattern for the calculation of the following configuration.

$$FE^2 = EA^2 + AB^2 + BF^2 - 2EA\cdot AB\cos(\theta_X + \theta_A) - 2EA\cdot BF\cos(\theta_X - \theta_B) + 2AB\cdot BF\cos(\theta_A + \theta_B) \quad (5)$$

Then, with the configuration of Figure 7, the analysis is carried out using trigonometric equations, from which Equations (6) to (10) are obtained.

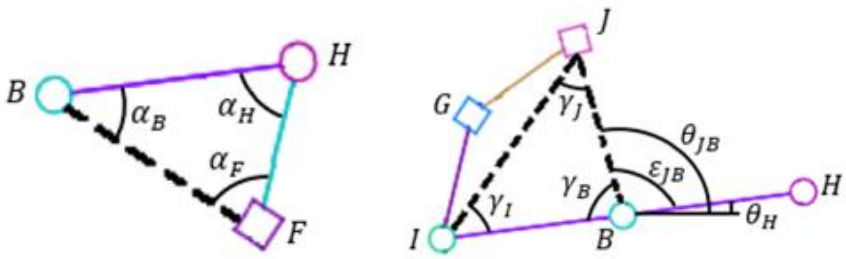

Figure 7. Bar configuration No 2.

$$HF^2 = BF^2 + BH^2 - 2\cdot BF\cdot BH\cdot\cos\alpha_B \quad (6)$$

$$\theta_H = \alpha_B - \theta_B \quad (7)$$

$$IJ^2 = BI^2 + BJ^2 - 2\cdot BI\cdot BJ\cdot\cos\gamma_B \quad (8)$$

$$\varepsilon_B = 180° - \gamma_B \quad (9)$$

$$\theta_{JB} = \varepsilon_B + \theta_H \quad (10)$$

Where *BI* equals 5 mm, *BJ* = 5 mm, *IJ* = 6.5 mm. We proceed with the analysis of the mechanism in Figure 8, which from Equations (11) to (15), allow us to obtain the value of θ_L which will be used in the following mechanism.

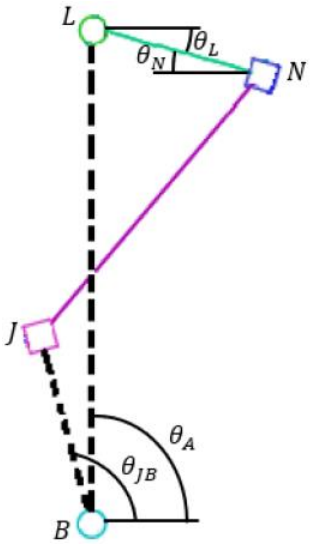

Figure 8. Bar configuration No 3.

$$BL\cos\theta_A + NL\cos\theta_L - JN\cos\theta_N - JB\cos\theta_{JB} = 0 \quad (11)$$

$$BL\sin\theta_A - NL\sin\theta_L - JN\sin\theta_N - JB\sin\theta_{JB} = 0 \quad (12)$$

$$JN^2\cos^2\theta_N = \left(BL\cos\theta_A + NL\cos\theta_L - JB\cos\theta_{JB}\right)^2 \quad (13)$$

$$JN^2\sin^2\theta_N = \left(BL\sin\theta_A + NL\sin\theta_L - JB\sin\theta_{JB}\right)^2 \quad (14)$$

$$N^2 = BL^2 + NL^2 + JB^2 + 2\cdot BL\cdot NL\cos(\theta_A + \theta_L) - 2BL\cdot JB\cos\left(\theta_A - \theta_{JB}\right) - 2NL\cdot JB\cos\left(\theta_L + \theta_{JB}\right) \quad (15)$$

Where JB equals 5 mm, NL = 5 mm, JN = 9.6 mm, and BL = 12.2 mm. Then, the mechanism of Figure 9 allows establishing equations to obtain the value of α_L, which determines the inclination of the fifth mechanism of bars raised in the configuration of the finger. These equations are described from (16) to (18).

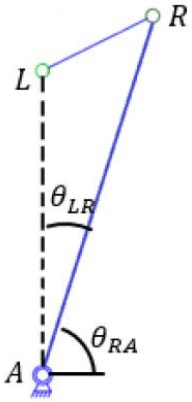

Figure 9. Bar configuration No 4.

$$\theta_{RA} = \theta_A - \theta_{LR} \quad (16)$$

$$AR\sin\theta_{RA} - AL\sin\theta_A = LR\sin\alpha_L \quad (17)$$

$$\alpha_L = \sin^{-1}\left(\frac{AR\sin\theta_{RA} - AL\sin\theta_A}{LR}\right) \quad (18)$$

Where AR equals 31.8 mm, AL = 28.3 mm, LR = 6.5 mm, and θ_{RA} 11°. Then, the fifth mechanism of Figure 10 is proposed in a four-bar cross configuration, in which the loop-closing and Freudenstein equation are implemented in Equations (19) to (24), to obtain the angular value of θ_W. This input value allows the sixth mechanism to locate the value of the distal phalanx end.

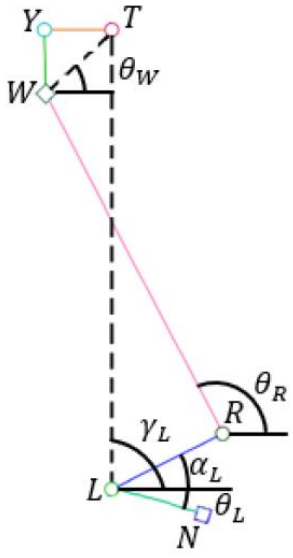

Figure 10. Bar configuration No 5.

$$\gamma_L = 90° - \theta_L \quad (19)$$

$$LR\cos\alpha_L + RW\cos\theta_R + WT\cos\theta_W - TL\cos\gamma_L = 0 \quad (20)$$

$$LR\sin\alpha_L + RW\sin\theta_R + WT\sin\theta_W - TL\sin\gamma_L = 0 \quad (21)$$

$$RW^2\cos^2\theta_R = (TL\cos\gamma_L - LR\cos\alpha_L - WT\cos\theta_W)^2 \quad (22)$$

$$RW^2\sin^2\theta_R = (TL\sin\gamma_L - LR\sin\alpha_L - WT\sin\theta_W)^2 \quad (23)$$

$$RW^2 = TL^2 + LR^2 + WT^2 + 2TL\cdot LR\cos(\gamma_L - \alpha_L) - 2TL\cdot WL\cos(\gamma_L - \theta_W) + 2LR\cdot WT\cos(\alpha_L - \theta_W) \quad (24)$$

Where LR equals 6.5 mm, RW = 20 mm, WT = 4.8 mm, and TL = 24 mm. Finally, the last mechanism in Figure 11 allows us to obtain the value in position of the point Q through the angular value of θ_Q, as described in Equations (25) and (26).

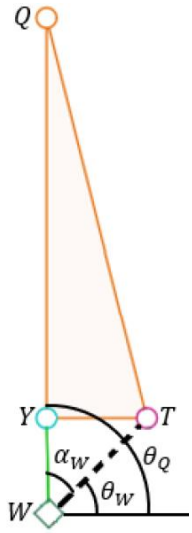

Figure 11. Bar configuration No 6.

$$YT^2 = WT^2 + WY^2 - 2WT\cdot WY\cos\alpha_W \quad (25)$$

$$\theta_Q = \theta_W + \alpha_W \quad (26)$$

Where WT equals 4.8 mm, WY = 3.3 mm, YT = 3.5 mm, and WQ = 17.3 mm.

Analysis of results

With the data obtained using the graphic method and kinematics analysis, the CAD design is made, and the trajectory is simulated by means of the SolidWorks program by carrying out a movement study, from which the behavior in Figure 12 is obtained.

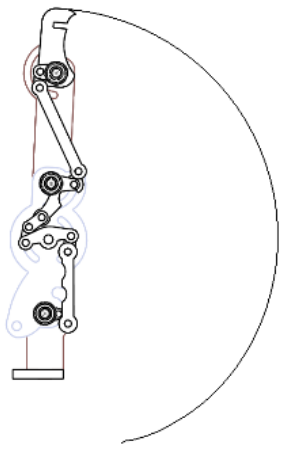

Figure 12. SolidWorks Trajectory.

These data are exported to Matlab and compared with those obtained in the ideal mechanism. Where the green trajectory in Figure 13 describes the behavior of a finger when its phalanges go from extension to flexion, and the blue trajectory the same route, but for the designed system.

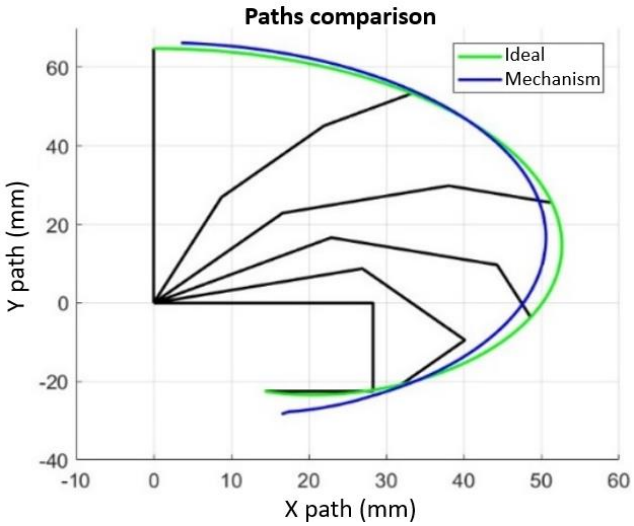

Figure 13. Path comparison.

The error generated by the ideal and real trajectories can be tolerated since the application of the mechanism is aimed at power grips, but not at precision grips.

To corroborate that the designed system has only one input variable, the degrees of freedom (F) of the system are calculated, according to the description in Figure 14 and the Grübler-Kutzbach Equation in (27).

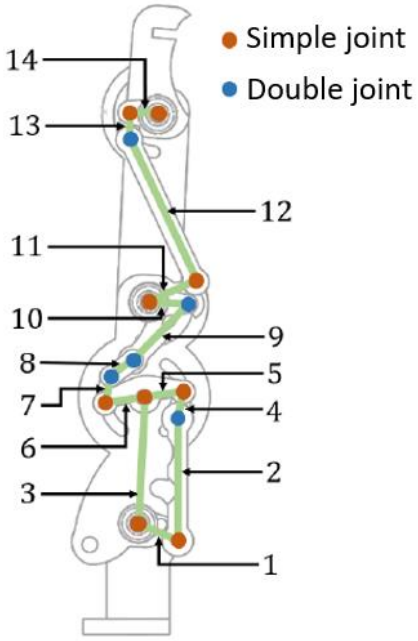

Figure 14. Calculation of degrees of freedom.

$$F = 3(n-1) - 2 \cdot p_v \quad (27)$$

Where n is the total number of links in the mechanism and p_v the number of joints acting in the two-dimensional plane. From the above, 14 links and 19 joints are obtained, both single and double, which with equation (27), determine one degree of freedom for the system.

Finally, the assembly of the five fingers of the hand is carried out with the crank handle type activation system in Figure 15. This gives the final system in Figure 16 in which the position of the hand is considered with ectrodactyly.

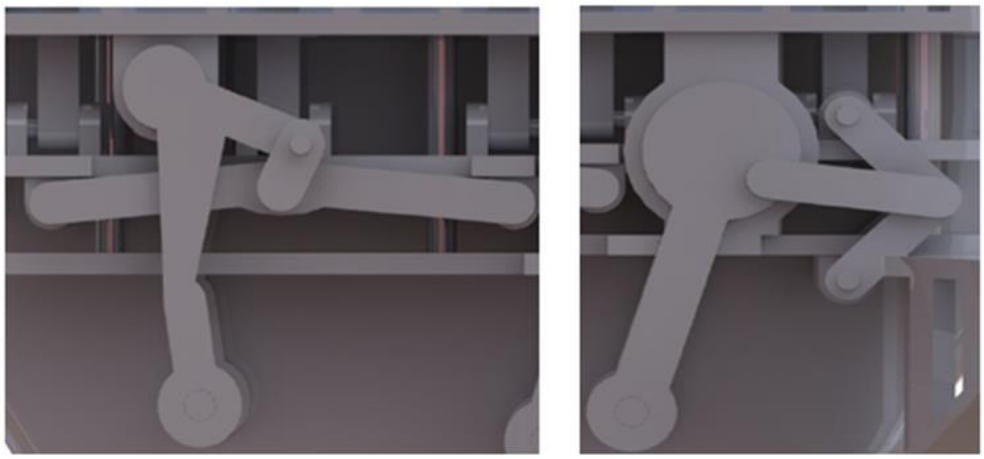

Figure 15. Activation system.

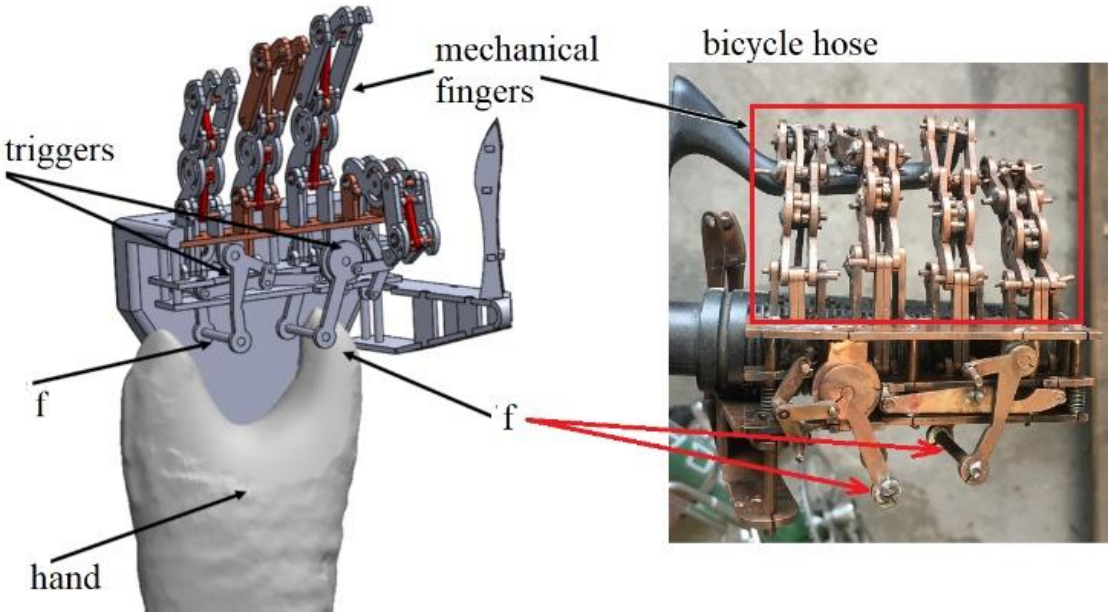

Figure 16. Final assembly.

Nomenclature

V/ble	Definition	V/ble	Definition
θ_A	angle of the bar AB	BF	distance between points B and F
θ_{RA}	angle of the bar AR	BJ	distance between points B and L
θ_H	angle of the bar BH	BL	distance between points B and J
θ_L , θ_N	angle of the bar NL	IJ	distance between points I and J
α_L	angle of the bar LR	JB	distance between points J and B
θ_R	angle of the bar RW	TL	distance between points T and L
θ_Q	angle of the bar YQ	WT	distance between points W and T
θ_B	angle of F with respect to B	AB	length of the bar AB
θ_{JB}	angle of B with respect to J	AR	length of the bar AR
θ_X	angle of A with respect to E	BH	length of the bar BH
θ_W	angle of W with respect to T	BI	length of the bar BI
θ_{LR}	angle between bar AR and points A and L	FE	length of the bar FE
α_B	angle between bar BH and points B and F	FH	length of the bar FH
ε_{JB}	angle between bar BH and points B and J	JN	length of the bar JN
γ_B	angle between bar BI and points B and J	LR	length of the bar LR
γ_L	angle between bar LR and points L and T	NL	length of the bar NL
α_W	angle between bar WY and points W and T	RW	length of the bar RW
F	Degrees of freedom	WY	length of the bar WY
AE	distance between points A and F	YT	length of the bar YT
AL	distance between points A and L	n	total of links
p_v	Total of 2D	p_v	total of 2D

Conclusion

This document aimed at developing the kinematic models and CAD software simulations of a bar mechanism for the construction of a hand that allows the generation of large diameter power grips, according to Cutkosky's taxonomy. These grips are characterized by having the fifth finger of the hand as fixed, so that the stipulated design does not present variations in the movement of the thumb. As for fingers 1 to 4, these must go from a state of extension to flexion from the angular variation of 0° to 90°, according to the hand goniometry; therefore, in the design the increase of each phalanx is made by one degree measured with respect to the previous one, this allows the fingers to reach the closing position in the same time interval.

On the other hand, the activation system for this angular variation is designed based on a lever handle type mechanism, which is operated by fingers one and five of the person with ectrodactyly. These fingers give a stroke of 15 mm, which is proportionally related to the stipulated angular variation, so that at the end of this movement the fingers reach their maximum angle of flexion.

Finally, a design that allows large diameter grips to be made for applications such as riding a bicycle or gripping elements with cross sections that not exceed 50 mm in diameter is obtained. These tasks should consider that the system actuates the fingers together and not individually. In addition, functionality of fingers 1 and 5 of the subject is maintained, avoiding possible muscle atrophy.

Acknowledgements

The development of this system was supported by the Universidad Militar Nueva Granada, from Colombia

References

Avila, G. A, (2018). Defectos Congénitos Colombia 2018. *Instituto Nacional de Salud.* Retrieved from https://www.ins.gov.co/buscador-eventos/Informesdeevento/DEFECTOS%20CONG%C3%89NITOS_2018.pdf

Belter, J. T., Segil, J. L., Dollar, A. M., & Weir, R. F. (2013). Mechanical design and performance specifications of anthropomorphic prosthetic hands: a review. *Journal of rehabilitation research and development*, *50*(5), 599-618. DOI: http://doi.org/10.1682/JRRD.2011.10.0188

Belter, J. T., Segil, J. L., Dollar, A. M., & Weir, R. F. (2013). Mechanical design and performance specifications of anthropomorphic prosthetic hands: a review. *The Journal of Rehabilitation Research and Development, 50*(5), 599-618. DOI: http://doi.org/10.1682/JRRD.2011.10.0188

Bharati, A., Navit, S., Khan, S. A., Jabeen, S., Grover, N., & Upadhyay, M. (2020). Ectrodactyly-ectodermal dysplasia clefting syndrome: a case report of its dental management with 2 years follow-up. *Case Reports in Dentistry*, *2020*(8418725), 5. DOI: https://doi.org/10.1155/2020/8418725

Cutkosky, M. R. (1989). On grasp choice, grasp models, and the design of hands for manufacturing tasks. *IEEE Transactions on Robotics and Automation*, 5(3), 269-279. DOI: http://doi.org/10.1109/70.34763

França Bisneto, E. N. (2012). Deformidades congênitas dos membros superiores: parte I: falhas de formação. *Revista Brasileira de Ortopedia, 47*(5), 545-552. DOI: http://doi.org/10.1590/S0102-36162012000500002

Gane, B. D., & Natarajan, P. (2016). Split-hand/feet malformation: a rare syndrome. *Journal of Family Medicine and Primary Care*, 5(1), 168-169. DOI: http://doi.org/10.4103/2249-4863.184656

Jabin, J., Adnan, E., Mahmud, S. S., Chowdhury, A. M., & Islam, M. R. (2019). Low cost 3D printed prosthetic for congenital amputation using flex sensor. In *Proceedings of the 5th International Conference on Advances in Electrical Engineering* [ICAEE] (p. 821-825). DOI: http://doi.org/10.1109/ICAEE48663.2019.8975415

Jindal, G., Parmar, V. R., & Gupta, V. K. (2009). Ectrodactyly/split hand feet malformation. *Indian Journal of Human Genetics*, *15*(3), 140–142. DOI: http://doi.org/10.4103/0971-6866.60191

Kalathia, M. B, Seta, A. A., & Parmar, P. N. (2013). A Case of ectrodactyly in a neonate. *Journal of Clinical Neonatology*, 2(3), 151–152. DOI: http://doi.org/10.4103/2249-4847.120013

Nirmala, S. V. S. G., Sandeep, C., Chaitanya, P., Nuvvula, S., & Veluru, S. (2015). Ectrodactyly: a rare anomaly of limbs. *Journal of Dr. NTR University of Health Sciences, 4*(1), 53-55. DOI: http://doi.org/10.4103/2277-8632.153329

Nunes, A. O., Jadan, P. V., & Bello, A. Z. (2014). Síndrome ectrodactilia-displasia ectodérmica y labio-paladar hendido (EEC), a propósito de un caso clínico. *Facultad de Ciencias Médicas, 17*(3), 40-42.

P&O MG LATAM. (2020*). Ectrodactilia y tratamiento prótesis de silicona*. Recovered from protesismg.com/cuales-son-las-malformaciones-y-anomalias-congenitas-de-la-mano/ectrodactilia_protesis_silicona/

Sutton, V. R., & Van Bokhoven, H. (1993). TP63-Related Disorders. *GeneReviews®*. Recovered on Juno 8, 2010, from https://pubmed.ncbi.nlm.nih.gov/20556892/

Valderrama-Zaldivar, L. J. (2013). Ectrodactilia; presentación de un caso. *Perinatología y Reproducción Humana, 27*(3), 200-204.

Van Der Niet, O., Bongers, R. M., & Van Der Sluis, C. K. (2013). Functionality of i-LIMB and i-LIMB pulse hands: case report. JRRD - *Journal of Rehabilitation Research & Development, 50*(8), 1123-1128. DOI: http://doi.org/10.1682/JRRD.2012.08.0140